# A numerical investigation of melt layer effects on hybrid combustion of liquefying fuels

Mohana Gurunadhan*, Varun Viswamithra, Shyam Menon, Keith Gonthier, Adam Baran
*Department of Mechanical Engineering, Louisiana State University, Baton Rouge, LA*

**During combustion of liquefying fuels in a hybrid propulsion system, the liquid film formed over the fuel surface can significantly affect the spatial regression rate by altering the streamwise vaporization rate induced by the bulk flow. In the current study, a simplified single-phase mathematical model is developed to describe how the liquid film affects vaporization for a Paraffin wax slab configuration. Numerical simulations are performed for inlet gaseous oxygen (GOX) mass fluxes of 16 $kg/(m^2s)$. Combustion is modeled using a mixing-limited Eddy Dissipation Model (EDM) with temperature-dependent thermophysical and transport properties. The relative fractions of mass transport by vaporization and transport by bulk flow of liquid in the film, due to gas shear, are analyzed and compared to data reported in the literature. Discrepancies between the predicted and measured trends for the streamwise spatial variation in regression rate along the fuel surface are highlighted and discussed. The spatial streamwise regression results demonstrate the importance of incorporating multiphase flow effects to accurately model the combustion of liquefying fuels in hybrid propulsion systems.**

## I. Introduction

A hybrid propulsion system provides an alternative to conventional solid and liquid systems. A review of the benefits of various hybrid propulsion systems is given in Ref. [1]. Conventional hybrid systems, using polymeric fuel, have the disadvantage of slower fuel regression rates. To overcome this disadvantage, recent hybrid systems that utilize liquefying hybrid fuels, capable of forming a distinct melt layer during combustion, have provided up to a 5 fold increase in regression rates. [1].

Experiments on liquefying fuels have been performed by various researchers [2] to examine the mechanism responsible for increased regression rates. An initial study attributed the observed rate increase to lower latent heats associated with liquefying fuels. Karabeyoglu et al.[3, 4] attributed the increased regression rate to a liquid melt layer surface instability and subsequent fuel droplet entrainment in the oxidizer flow which was corroborated by the previous experiments of Gater et al.[5]. The study of Karabeyoglu motivated combustion experiments focused on fuel entrainment.

Nakagawa et al.[6] and Chandler et al's [7] experiment obtained images, showing droplet motion and ligament-like formation during combustion tests. In a similar work, Jens et al. [8] obtained images for the combustion of paraffin wax slabs at elevated pressure, which showed substantial fuel melt liquid displacement and transport. In a recent work, Petrarolo [9] performed experiments on combustion of paraffin wax, to characterize instability of liquid melt layer. Most of the aforementioned experimental studies could not capture melt film thickness or droplet entrainment mechanism.

Due to experimental limitations, it is important to develop computational models capable of simulating hybrid fuel combustion. From a large collection of computational works in Hybrid combustion, notable computational efforts are the work of Coronneti et al. [10] (HTPB) and Leccesse et al. [11] (Paraffin wax), which included relevant kinetic-rate chemistry in hybrid rocket combustion. Computational studies in Hybrid combustion, were mostly limited to single phase conditions and the fuel phase change- solid-liquid (liquefying fuels) & solid-vapor (Polymeric fuel), during combustion, were not treated explicitly.

The main goal of our research is to computationally model the coupled turbulent combustion-melting problem and examine the relative effects of vaporization, liquid entertainment and stream

*Questions: mgurun1@lsu.edu

wise variation of fuel regression, on the averaged regression rate and ensuing combustion. To that end, in the current work, single phase simulations are conducted, considering the effect of melt film thickness on rate of melting and rate of vaporization. The current study is conducted to understand the adequacy of single phase simulations and necessity for conducting a detailed Multiphase simulation. The current paper is structured as follows- The computational methodologies, employed for modeling pertinent physics, are detailed in Section.2. The geometry of the computational domain and simulated operating conditions are listed in Section.3 and the representative results are discussed in Section.4.

## II. Methodology

The three essential aspects of single phase computational model are flow-turbulence, turbulence-chemistry interaction and radiation. The methodology chosen, for each of the fore mentioned physics, is not only based on its relevance and accuracy, but also based on its compatibility with other pertinent physics. For the flow-turbulence physics, considering the potential computational load and the pursued combustion flow field, two equation SST k-w model is preferred over detailed Large Eddy Simulation (LES) and Direct Numerical Simulation (DNS). The flow channels and configurations, of interest to the propulsion community, can be sufficiently modeled using basic RANS equation.

The second aspect of central importance is the interaction between turbulence and chemical reaction (combustion). In the work of Magnussen et. al [12], it was proposed that for cases with fast Arrhenius reaction rates(compared to mixing scale), the rate of combustion will be determined by the rate of dissipation of turbulent eddies (mixing time scale). This method is referred to as the Eddy Dissipation Method (EDM) and is employed in the current work.

To include the effects of vaporization in single phase flow, an in-house Parallel User Defined Function (UDF) was developed, with the capability to handle complete vaporization conditions from evaporation to boiling. The algorithm considers the energy, mass balance at the fuel surface and evaluates the rate of vaporization. The vaporization rate is imposed as volumetric source term in the cell adjacent to the fuel surface. The liquid-gas interfacial Mass Balance (MB) and Energy Balance (EB) can be defined as,

$$\textbf{Mass Balance:} \quad \omega_v \left(1 - Y_{I,f}\right) = \rho_{\mathrm{g}} D_{\mathrm{fg}} \left.\frac{\partial Y_f}{\partial n}\right|_I \tag{1}$$

$$\textbf{Energy Balance:} \quad \omega_v H_v = \underbrace{\kappa_{\mathrm{g}} \left.\frac{\partial \mathrm{T}}{\partial n}\right|_g - \kappa_{\mathrm{l}} \left.\frac{\partial \mathrm{T}}{\partial n}\right|_l}_{q^{"}_{\mathrm{net,c}}} + \underbrace{\mathrm{q}_{\mathrm{rad,i}} - \mathrm{q}_{\mathrm{rad,e}}}_{q^{"}_{\mathrm{net,r}}} \tag{2}$$

where subscript $l$, $s$, $g$ and $v$ indicates liquid, solid, gas mixture and vapor phase properties, respectively, while subscript $I$ refers to the properties evaluated at liquid-gas interface. The partial derivative in mass balance equation represents the normal gradient of gaseous fuel mass fraction. $Y_f^I$ represents the fuel mass fraction at the interface, whose value is related to the vapor pressure $P_f^I$, similar to the work of Tanguy et. al [13], $H_v$ represents the latent heat of vaporization and $\omega_v$ represents the vaporization mass flux.

For the vaporization problem, an iterative technique is used to evaluate the vaporization rate ($\dot{r}_v$). In this technique, the energy and mass balance equations are combined as,

$$\dot{r}_{v,\mathrm{int}} = \frac{Y_{I,f}}{\mathrm{L_f}\rho_{\mathrm{l}}} \left\{ q^{"}_{\mathrm{net,c}} + q^{"}_{\mathrm{net,r}} \right\} - \rho_{\mathrm{g}} D_{\mathrm{fg}} \frac{\partial Y_f}{\partial n} \tag{3}$$

$\dot{r}_{v,\mathrm{int}}$ represents the intermediate vaporization rate in the iterative procedure, whichis used to evaluate

| Physics | Model/ Technique |
|---|---|
| **Turbulence** | SST k-$\omega$ model |
| **Multiphase** | Implicit VOF with compressive scheme |
| **Combustion** | Eddy- Dissipation Method |
| **Radiation** | Discrete Ordinate Method (DOM) |

**Table 1** Summary of computational models

| **PARAMETER** | **INPUT VALUES** |
|---|---|
| Domain Dimension [mm] | $L_i$ = 217.5, $L$ = 400 $H$ = 25.4 |
| **INITIAL CONDITIONS** | |
| Dimension (Fuel slab) [mm] | $L_m$ = 73&$H_m$ = 9 |
| **BOUNDARY CONDITIONS** | |
| Oxidizer mass flux $\left[\frac{kg}{m^2 s}\right]$ | $G_o$ = 16&40 |
| Pressure [Pa] | 101325 |
| Inlet temperature [K] | 300 |

**Table 2** Input parameters for the simulation

the corrected interface temperature, defined as,

$$T_{I,\mathrm{cor}} = \frac{\left\{-\kappa_{\mathrm{g}}\dfrac{\mathrm{T_{I,g}}}{\Delta n} - \kappa_{\mathrm{l}}\dfrac{\mathrm{T_{I,l}}}{\Delta n} - q''_{\mathrm{net,r}}\right\}}{\dfrac{-\kappa_{\mathrm{g}}}{\Delta n} - \dfrac{-\kappa_{\mathrm{l}}}{\Delta n}} \tag{4}$$

The Eq. (4) and Eq. (3) are solved iteratively until the convergence of vaporization rate ($\dot{r}_v$) and ($T_I$). In the iterative procedure, the interface cell temperature is used as the initial interface temperature. In the iterative procedure, $\dot{r}_{v,\mathrm{int}}$ value is under relaxed before its application in Eq. (4), which significantly improves the convergence rate. As mentioned earlier, the converged vaporization rate is imposed as a interfacial mass $S_I$ and energy source term $S_E$ , defined as,

$$\mathrm{S}_I = \dot{r}_v \rho_l \frac{A_I}{\mathrm{V}_{cell}} \quad \mathrm{S}_E = -\mathrm{S}_I \mathrm{L_v} \tag{5}$$

where $A_I$ is the area of interface and $\mathrm{V}_{cell}$ is the volume of the interface cell.

The final aspect of the problem is radiation. Discrete Ordinate Model (DOM) is preferred for radiation, considering the possibility of low radiation optical thickness. The pertinent details of the computational model are listed in Table. 1. The scope of the current study is limited to analyzing the effect of liquid film on fuel regression. The liquid film thickness can have a significant contribution to the heat transfer at Solid-Liquid (SL) and Liquid-Gas (LG) interface, affecting the LG interface temperature, rate of vaporization and rate of melting. In a single phase simulation, the presence of liquid film can mathematically modeled through the interfacial heat balance equation. The normal co-ordinate of the fuel surface (wall) in Fig. 1a, is assumed to be the LG interface normal, which is a valid assumption when the film thickness ($\delta_l$) to slab length ($L_m$) ratio is small $\left(\dfrac{\delta_l}{L_m}\right) << 1$. To understand the sensitivity of film thickness, three cases are considered. In the first case (Case-1), the presence of film thickness is neglected and the heat loss ($\dot{Q}_{loss}$ due to melting was modeled as,

$$\dot{Q}_{loss} = \underbrace{\frac{\overline{\dot{r_m}}}{\kappa_s}(T_m - T_a)}_{\dot{Q}_s} + \rho_s H_m \dot{r_m} \tag{6}$$

where $\dot{Q}_s$ represents heat lost to the solid fuel, with its expression derived using a one-dimensional analysis, similar to the work of Karabeyoglu [3] and $\overline{\dot{r_m}}$ represents the spatial average regression rate. For the second case (Case-2), a constant liquid film thickness was assumed, using the thickness equation provided in the work of Karabeyoglu [3], derived based on the assumption of high radiation absorption coefficient of the liquid film. The evolution of liquid film thickness is explicitly modeled in the third case (Case-3), while considering a simplified momentum equation. Using the lubrication approximation, assuming a shear driven flow, the x-momentum equation can be simplified as,

$$\frac{\partial}{\partial y}\left(\mu_l \frac{\partial u}{\partial y}\right) = 0 \tag{7}$$

Using gas shear $\tau_g$ on the vaporizing interface (wall) Fig. 1a as B.C., the above equation results in a

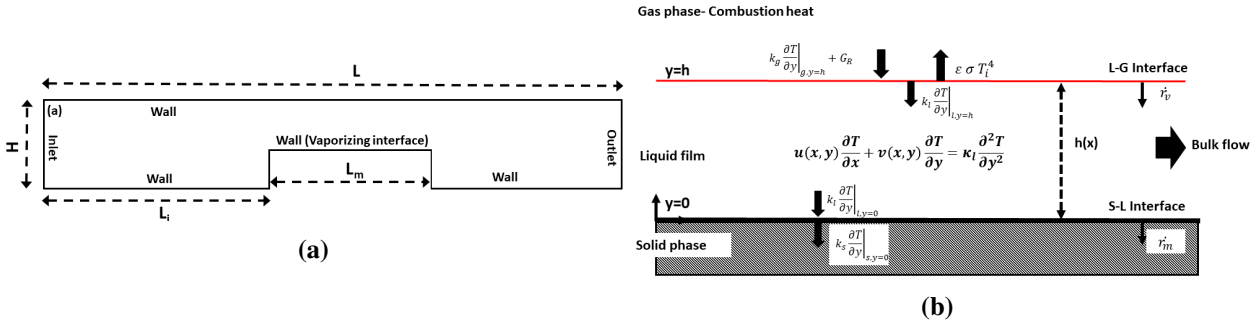


**Fig. 1** (a) Computational domain (b) Schematic of heat transfer at the Liquid-Gas (LG) and Solid- Liquid (SL) interface

linear profile for x-velocity. Integrating the two dimensional continuity equation in the y-direction and using the kinematic boundary condition at the LG interface, the governing equation for liquid film thickness can be expressed as,

$$\frac{\partial}{\partial x}\left(\frac{\tau_g \delta_l^2}{2\mu_l}\right) = \overline{\dot{r_m}} - \dot{r_v} \tag{8}$$

For Case-2 and Case-3, temperature in the liquid film was expressed as [3],

$$T_l = \frac{\overline{\dot{r_m}}}{\kappa_l} \frac{(T_m - T_I)}{\left(1 - \exp\left(\frac{\overline{\dot{r_m}}\delta_l}{\kappa_l}\right)\right)} \left\{\exp\left(\frac{\overline{\dot{r_m}}y}{\kappa_l}\right) - \frac{\overline{\dot{r_m}}}{\kappa_l} + T_m\right\} \tag{9}$$

## III. Computational domain and Operating conditions:

The computational domain dimensions, initial and operating conditions are adopted from the work of Dunn et. al [14], as listed in Table.2. For meshing, a static biased mesh is employed, wherein mesh is refined at the wall surface, such that the normalized distance $Y^+$ of the cell adjacent to the wall, is ensured to be $\leq 1$ [15]. The simulations were conducted on computational domain discretized to $\approx 0.45$ million cells. The paraffin wax fuel (mixture of hydrocarbons) is represented by $C_{32}H_{66}$ hydrocarbon [11]. Based on the work of Leccese et. al [11], $C_{32}H_{66}$ hydrocarbon is assumed to thermally crack into Ethylene ($C_2H_6$) and the combustion is modeled as single step equilibrium reaction of Ethylene (NASA CEA). The details of the reaction are given below:

$$C_{32}H_{66} \rightarrow 16C_2H_6 + H_2$$

$$C_2H_6 + 2.025O_2 \rightarrow 1.24CO + 0.76CO_2 + 1.29H_2O + 0.71H_2$$

## IV. Results

Four parameters are chosen to analyze the effect of film thickness- temperature distribution normal (Y) to the fuel surface at the mid section Fig. 2a, the flame position Fig. 2b, regression rate Fig. 3a and temperature Fig. 3b of fuel surface, along the stream wise direction (X). The X-coordinate is normalized with length of the slab, with the X-Y origin located at leading edge of fuel slab surface (wall) Fig. 1a. The step changes noticed in flame position, Fig. 2b, and interface temperature, Fig. 3b, can be attributed to mesh resolution, $O(0.1mm)$, in the flow region away from the wall. From the regression rate and slab temperature, Case-1 has the lowest average melting rate and highest slab temperature , wherein Case-1 is based on the assumption that vaporization rate ($\dot{r}_v$) is equal to the melting rate ($\dot{r}_m$), neglecting the film thickness. In comparison to the Vaporization rates of other cases, Case-1 has the highest Vaporization rate. This behavior is expected, as the presence of liquid film is neglected in Case-1, which reduces the rate of heat loss from the LG interface,

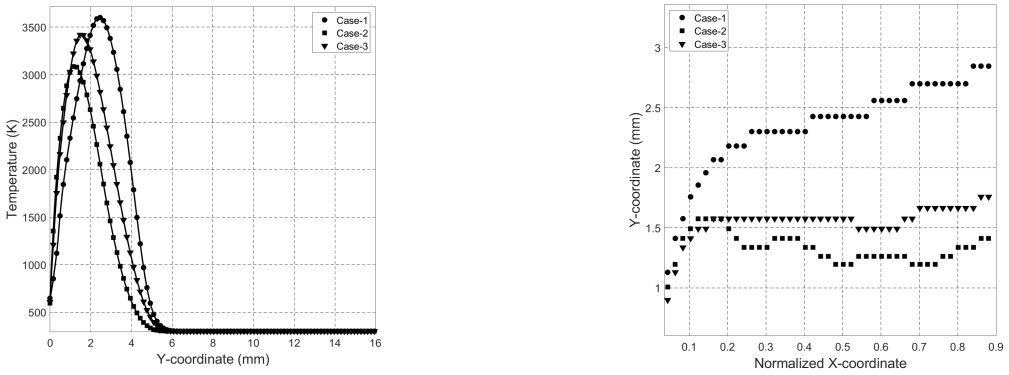


**(a)** **(b)**

**Fig. 2** (a) Normal temperature distribution at slab center line (b) Flame position along the fuel surface

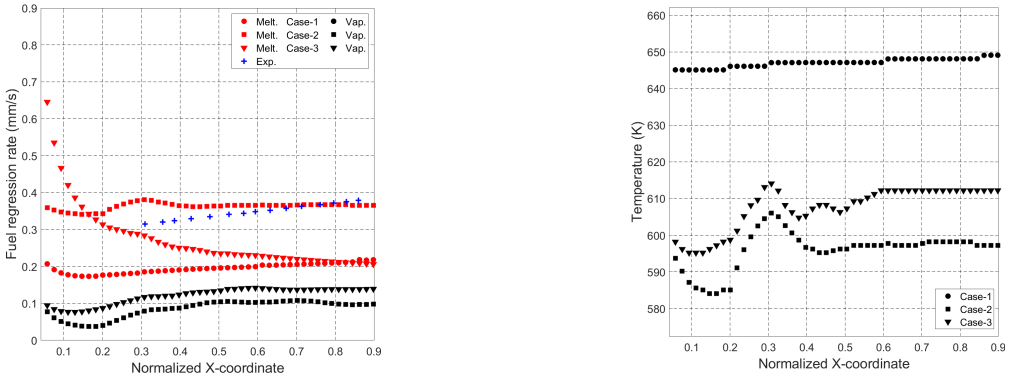


**(a)** **(b)**

**Fig. 3** (a) Fuel regression along the fuel slab (b) Interface temperature

resulting in a higher interface temperature. Higher vaporization rate results in displacement of flame position,identified as the peak temperature point, away from the fuel surface, reducing the temperature and mass fraction gradient at the interface. For Case-2, constant (spatial) film thickness is imposed, which reflects in the corresponding regression rate. The regression rate fluctuations of Case-2 Fig. 3a is caused by fluctuation in gas temperature and associated gradients. In Case-3, the stream wise evolution of film thickness is modeled and the effect of spatially varying film thickness on regression rate is included. The melt film is expected to have lowest melt film thickness at the leading edge, growing in the stream wise direction, which is reflected in their melting rates, wherein the leading edge has the highest rate of melting. The fraction of melt being vaporized is observed to be $\approx 25\%$ and $\approx 55\%$ for Case-2 and Case-3. Since melt film thickness is maintained a constant for Case-2, the vaporization fraction will not be indicative of the actual behavior and hence can be neglected. From the case-3 regression rates, mass transport by bulk flow (Melting-vaporization rate) constitutes a major fraction of the total melting rate. The streamwise regression rates observed in the experiment of Dunn et. al [14] is overlayed in Fig. 3a, for comparison. As the experimental regression rate was measured by Shadowgraphy, it can be interpreted as the stream wise melting rate. From Fig. 3a a difference is observed between the experimental and numerical melting rates, in terms of its spatial trend and mean value. Two probable reasons for the observed difference are:

- Inadequacy of the simplified film model employed in the current work, in capturing the actual variation of melt film thickness.
- In a physical problem, smoothening of sharp corner, due to higher melting rate at the leading edge, as observed in Case-3, can modify the gas flow field and the convective heat transfer rates.

Numerical verification of the fore mentioned reasons necessitate a multiphase simulation,

including SL phase change. The multiphase simulation can also provide inputs for development of simplified melting model, for incorporation in single phase combustion studies.

## V. Conclusion

In the present work, the single phase numerical simulation of a hybrid propulsion system was conducted with Paraffin wax fuel. The sensitivity of liquid film thickness on melting/ vaporization rate was studied, by using three different modifications heat balance equation at Liquid-Gas interface. From the simulation results, it is observed that the vaporization and melting rates are highly sensitive to liquid film thickness and associated heat loss. The liquid melt removal by bulk flow (gas shear), constitutes a major fraction of total melting, in comparison to the mass transferred by vaporization. A theoretical explanation for the observed difference between simulations and experiments, justifies development of a detailed Multiphase combustion model, including Solid-Liquid phase change.

## References


[1] Kuo, K. K., and Chiaverini, M. J., *Fundamentals of hybrid rocket combustion and propulsion*, American Institute of Aeronautics and Astronautics, 2007.

[2] Larson, C., DeRose, M., Pfeil, K., Carrick, P., DeRose, M., Pfeil, K., Carrick, P., and Larson, C., "Tube burner studies of cryogenic solid combustion," *33rd Joint Propulsion Conference and Exhibit*, 1997, p. 3076.

[3] Karabeyoglu, M., Altman, D., and Cantwell, B. J., "Combustion of liquefying hybrid propellants: Part 1, general theory," *Journal of Propulsion and Power*, Vol. 18, No. 3, 2002, pp. 610–620.

[4] Karabeyoglu, M., and Cantwell, B. J., "Combustion of liquefying hybrid propellants: Part 2, Stability of liquid films," *Journal of Propulsion and Power*, Vol. 18, No. 3, 2002, pp. 621–630.

[5] Gater, R. A., and L'Ecuyer, M. R., "A fundamental investigation of the phenomena that characterize liquid-film cooling," *International Journal of Heat and Mass Transfer*, Vol. 13, No. 12, 1970, pp. 1925–1939.

[6] Nakagawa, I., and Hikone, S., "Study on the regression rate of paraffin-based hybrid rocket fuels," *Journal of Propulsion and Power*, Vol. 27, No. 6, 2011, pp. 1276–1279.

[7] Chandler, A., Jens, E., Cantwell, B., and Hubbard, G. S., "Visualization of the liquid layer combustion of paraffin fuel for hybrid rocket applications," *48th AIAA Joint Propulsion Conference & Exhibit*, 2012, p. 3961.

[8] Jens, E. T., Chandler, A. A., Cantwell, B., Hubbard, G. S., and Mechentel, F., "Combustion visualization of paraffin-based hybrid rocket fuel at elevated pressures," *50th AIAA Joint Propulsion Conference*, 2014, p. 3848.

[9] Petrarolo, A., Kobald, M., and Schlechtriem, S., "Optical analysis of the liquid layer combustion of paraffin-based hybrid rocket fuels," *Acta Astronautica*, Vol. 158, 2019, pp. 313–322.

[10] Coronetti, A., and Sirignano, W. A., "Numerical analysis of hybrid rocket combustion," *Journal of Propulsion and Power*, Vol. 29, No. 2, 2013, pp. 371–384.

[11] Leccese, G., Bianchi, D., and Nasuti, F., "Modeling and Simulation of Paraffin–Based Hybrid Rocket Internal Ballistics," *2018 Joint Propulsion Conference*, 2018, p. 4533.

[12] Magnussen, B. F., and Hjertager, B. H., "On mathematical modeling of turbulent combustion with special emphasis on soot formation and combustion," *Symposium (international) on Combustion*, Vol. 16, Elsevier, 1977, pp. 719–729.

[13] Tanguy, S., Ménard, T., and Berlemont, A., "A level set method for vaporizing two-phase flows," *Journal of Computational Physics*, Vol. 221, No. 2, 2007, pp. 837–853.

[14] Dunn, C., Gustafson, G., Edwards, J., Dunbrack, T., and Johansen, C., "Spatially and temporally resolved regression rate measurements for the combustion of paraffin wax for hybrid rocket motor applications," *Aerospace Science and Technology*, Vol. 72, 2018, pp. 371–379.

[15] Wilcox, D. C., et al., *Turbulence modeling for CFD*, Vol. 2, DCW industries La Canada, CA, 1998.